Probing the Sensory Rhodopsin II Binding Domain of its Cognate Transducer by Calorimetry and Electrophysiology

ARTICLE *in* JOURNAL OF MOLECULAR BIOLOGY · AUGUST 2003

Impact Factor: 4.33 · DOI: 10.1016/S0022-2836(03)00656-9 · Source: PubMed

9 AUTHORS, INCLUDING:

Johann P Klare
Universität Osnabrück
84 PUBLICATIONS **1,783** CITATIONS
SEE PROFILE

Georg Nagel
University of Wuerzburg
72 PUBLICATIONS **6,906** CITATIONS
SEE PROFILE

doi:10.1016/S0022-2836(03)00656-9 J. Mol. Biol. (2003) 330, 1203–1213

JMB

Available online at www.sciencedirect.com

SCIENCE DIRECT®

Probing the Sensory Rhodopsin II Binding Domain of its Cognate Transducer by Calorimetry and Electrophysiology

Silke Hippler-Mreyen[1], Johann P. Klare[1], Ansgar A. Wegener[1] Ralf Seidel[1], Christian Herrmann[2], Georg Schmies[3], Georg Nagel[3] Ernst Bamberg[3] and M. Engelhard[1]*

[1]*Department of Physical Biochemistry Max-Planck-Institute of Molecular Physiology Otto-Hahn-Straße 11, D-44227 Dortmund, Germany*

[2]*Department of Structural Biology, Max-Planck-Institute of Molecular Physiology Otto-Hahn-Straße 11, D-44227 Dortmund, Germany*

[3]*Department of Biophysical Chemistry Max-Planck-Institute of Biophysics, Kennedyallee 70 D-60596 Frankfurt/Main Germany*

**Corresponding author*

Sensory rhodopsin II, a repellent phototaxis receptor from *Natronobacterium pharaonis* (NpSRII) forms a tight complex with its cognate transducer (NpHtrII). Light excitation of the receptor triggers conformational changes in both proteins, thereby activating the cellular two-component signalling cascade. In membranes, the two proteins form a 2:2 complex, which dissociates to a 1:1 heterodimer in micelles. Complexed to the transducer sensory rhodopsin II is no longer capable of light-driven proton pumping. In order to elucidate the dimerisation and the size of the receptor-binding domain of the transducer, isothermal titration calorimetry and electrophysiological experiments have been carried out. It is shown, that an N-terminal sequence of 114 amino acid residues is sufficient for tight binding ($K_d = 240$ nM; $\Delta H = -17.6$ kJ mol^{-1}) and for inhibiting the proton transfer. These data and results obtained from selected site-directed mutants indicate a synergistic interplay of transducer transmembrane domain (1–82) and cytoplasmic peptide (83–114) leading to an optimal and specific interaction between receptor and transducer.

Keywords: association constant; thermodynamics of membrane proteins; isothermal titration calorimetry; voltage clamp; phototaxis

Introduction

Archaeal phototaxis is mediated by the two sensory rhodopsins SRI and SRII (also named phoborhodopsin[1]). These two photoreceptors are closely related to the two ion pumps bacteriorhodopsin (BR) and halorhodopsin (HR). They consist of seven transmembrane helices and a retinal chromophore attached to the protein *via* a protonated Schiff base with a conserved Lys residue. They share not only structural homologies but also functional properties like e.g. light-driven ion translocation (for recent reviews, see Schäfer *et al.*,[2] Sasaki & Spudich,[3] Lanyi[4] and Haupts *et al.*[5]). SRI enables the bacteria to seek light conditions optimal for the function of the light-driven ion pumps HR and BR and to avoid ultraviolet light. The second photoreceptor SRII conveys negative phototaxis, the physiological function of which has not yet been unequivocally established but might enable the bacteria to evade harmful conditions of high oxygen concentrations in the presence of light.[6] Both receptors are bound to membrane proteins (halobacterial transducers of rhodopsins; HtrI, HtrII) consisting of a two-helical transmembrane and a coiled/coil cytoplasmic domain. HtrII from *Halobacterium salinarum* (HsHtrII) possesses also an extracellular domain, which functions as a Ser receptor.[7] Photoexcitation of the receptor leads to an activation of the cytoplasmic domain of the corresponding transducer, which in turn triggers a signalling cascade. This signal transduction chain, which is homologous to the eubacterial two-component chemotaxis system (reviewed by Falke *et al.*[8] and Stock *et al.*[9]) regulates the switch

S.H-M. and G.S. contributed equally to this work.

Abbreviations used: HtrII, rhodopsin transducer II; HsHtrII, HtrII from *H. salinarum*; NpHtrII, HtrII from *N. pharaonis*.

E-mail address of the corresponding author: martin.engelhard@mpi-dortmund.mpg.de

frequency of the flagellar motor and the adaptation of the bacteria to constant stimuli (reviewed by Hoff *et al.*[10] and Marwan & Oesterhelt[11]).

The activation of SRII from *Natronobacterium pharaonis* (NpSRII) by light induces a photocycle with intermediates quite similar to those of BR although the turnover is two orders of magnitude slower.[12] The photocycles of both BR and NpSRII contain an M intermediate, whose formation coincides with the deprotonation of the Schiff base and the release of a proton from the extracellular channel. The decay of M and the formation of the original ground state correlate with the uptake of a proton from the cytoplasm and the reprotonation of the Schiff base.[13,14] The fast turnover of BR leads to an efficient proton pump, whereas the slow photocycle of NpSRII makes this rhodopsin a poor if at all vectorial proton pump.[15]

Structural information for sensory rhodoposin II from *N. pharaonis* (NpSRII) and for its complex with the transducer fragment NpHtrII-114 is now available. From the crystal structure analysis Luecke and co-workers anticipated that Tyr199 of the receptor is specifically involved in transducer binding,[16] a projection that was verified in the crystal structure of the NpSRII/NpHtrII complex.[17] In another publication Royant *et al.* pointed to a patch of positive charges on helix F which might bind a peptide from the transducer containing a cluster of negative charges (Gly^{100}AspGlyAspLeuAsp).[18] In the crystal structure of the complex this segment of the transducer is not resolved.[17]

The binding interface between NpSRII and NpHtrII is formed by helix F and G as well as TM1 and TM2, respectively (see Figure 1). From these data and earlier work using EPR spectroscopy[19,20] it was concluded that on light excitation helix F induces in a flap-like movement a rotary motion of TM2. One of the EPR-reporter groups replaced V78, therefore the changes in mobility are observed at a site that is only one helix turn apart from the border between structurally resolved (L82) and unresolved segments of the transducer. Consequently, without further information on the structure of the C-terminal peptide it becomes difficult to elucidate the molecular mechanism of signal transduction from the membrane domain to the cytoplasmic signalling domain.

In order to determine the size of the receptor-binding domain of the transducer, two different kinds of experiments have been performed. In the first series of experiments the dissociation constant (k_D) of the shortened transducers to the receptor has been measured by isothermal titration calorimetry. In a second part the observation that NpHtrII blocks the inherent proton pump of NpSRII[21,22] has been utilised to narrow the necessary size of the binding domain for efficient inhibition of the proton pump. These experiments were done by expressing both NpSRII and shortened NpHtrII fragments in *Xenopus* oocytes,

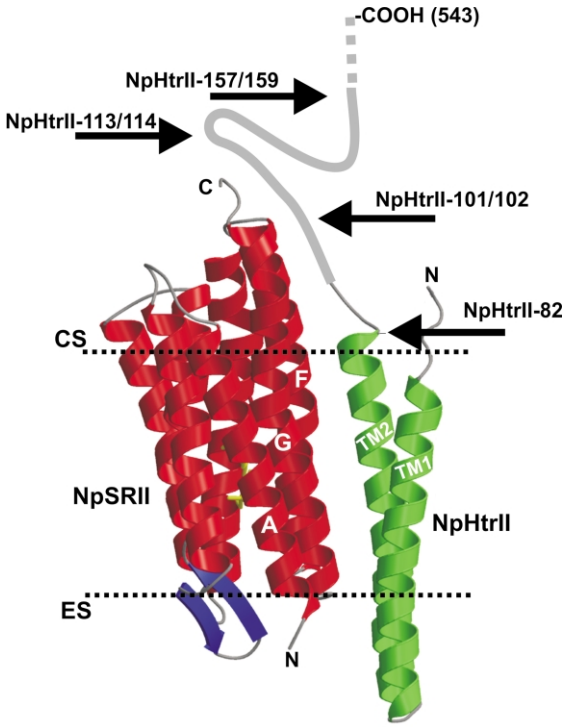

Figure 1. The crystal structure of NpSRII and NpHtrII (Protein Data Bank accession code 1H2S[17]). Helices A, F and G of the receptor (red ribbons) and the TMs of the transducer (green ribbons) are labelled. The dotted lines confine the major hydrophobic portion of the proteins. The cytoplasmic (CS, top) and extracellular (ES, bottom) sides of the membrane are labelled. The cytoplasmic domain, for which structural data do not exist, is symbolised by a grey thread. The position of the C terminus of the respective truncated transducer molecules is indicated by the labelled arrows.

which provides the possibility to study under voltage clamp conditions the light-activated proton transfer across the cellular membrane.[22,23] The results described here indicate that NpHtrII-114 is the smallest fragment that is still capable of binding efficiently to the receptor as well as of blocking the proton pump activity. Furthermore, the data provide insight into the thermodynamics and kinetics of membrane protein interactions.

Results

Expression and purification of NpSRII, NpHtrII, and NpHtrII analogues

NpSRII, NpHtrII, NpHtrII-157, NpHtrII-114, NpHtrII-101, and NpHtrII-82 were expressed as C-terminal His-tag fusion proteins in *Escherichia coli*.[24,25] Figure 2(a) shows the Coomassie-stained gel of the total cell lysates expressing NpHtrII (lane 3, before induction; lane 4, after induction) and NpHtrII-157 (lane 1, before induction; lane 2, after induction). In Figure 2(b) the corresponding Western-blot analysis using a polyclonal antibody

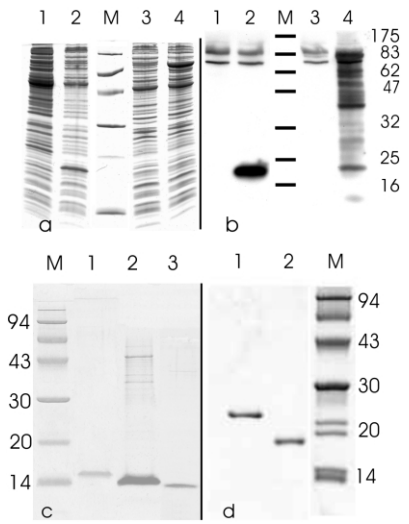

Figure 2. Electrophoretic analysis of the protein expressions. a, Coomassie-stained SDS/polyacrylamide gel of total cell lysates before and after induction with 1 mM IPTG (lanes 1 and 2 for NpHtrII-157 and 3 and 4 for NpHtrII-full-lengh). b, Corresponding Western blot using a self-made polyclonal antibody (rabbit) against the cytoplasmic portion of NpHtrII (77–149). c and d, SDS-PAGE-analysis of the transducer fragments after purification by Ni-NTA affinity (c) and DEAE chromatography (d). Lane 1 shows the purified transducer fragment NpHtrII-114; lane 2, NpHtrII-101; and lane 3, NpHtrII-82. Lanes 1 and 2 in (d) correspond to the purified receptor NpSRII and the transducer fragment NpHtrII-157, respectively.

(rabbit) against the sequence of NpHtrII comprising amino acid residues 77–149 is shown. The polyclonal antibody is not entirely specific, as obvious from the bands at around 80 kDa (Figure 2(b), lanes 1–3). The blot also reveals that during the induction and preparation of the whole cell lysate NpHtrII is degraded by proteolysis (Figure 2(b), lane 4). Since the polyclonal antibodies are directed towards epitopes close to the membrane domain of NpHtrII, all bands represent N-terminal fragments. The smallest band is approximately of the same size as NpHtrII-157.

The proteins were purified from solubilised membrane fractions by Ni-NTA chromatography with yields about 1–2 mg/l culture. An SDS/polyacrylamide gel of the purified proteins is shown in Figure 2(c) (lane 1, NpHtrII-114, 13–15 kDa; lane 2, NpHtrII-101, 12–13 kDa; lane 3, NpHtrII-82, 10–11 kDa) and Figure 2(d) (lane 1, NpSRII, 25 kDa; lane 2, NpHtrII-157, 18 kDa).

Formation of the NpSRII/NpHtrII complex *in vitro*

In order to investigate the binding of transducer fragments to NpSRII, blue-native polyacrylamide gel electrophoresis (BN-PAGE)[26] was performed. In a typical experiment the transducer was mixed with increasing amounts of NpSRII. Figure 3(a) shows the result for NpHtrII-157. There are three

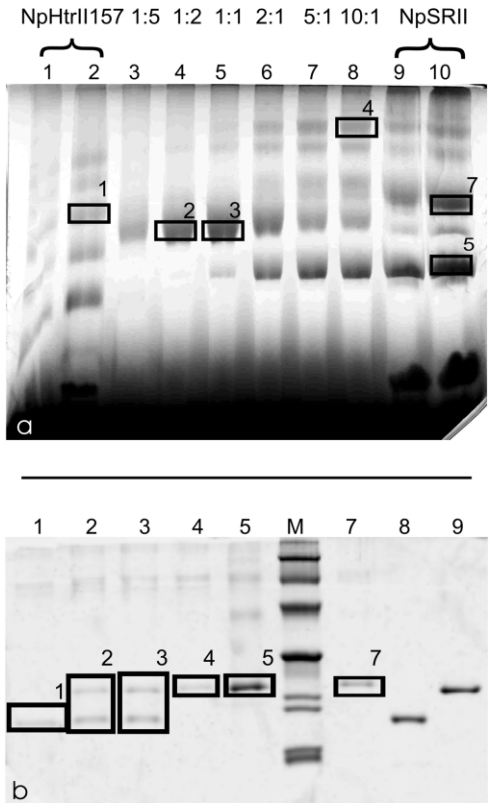

Figure 3. BN-PAGE of NpSRII and NpHtrII-157 at different concentrations (a). The receptor and the transducer were applied as references in lanes 1, 2 and 9, 10, respectively. The solubilised proteins NpSRII and NpHtrII-157 were mixed at molar ratios of 1:5 (lane 3), 1:2 (lane 4), 1:1 (lane 5), 2:1 (lane 6), 5:1 (lane 7), and 10:1 (lane 8). After incubation of the samples for one hour at room temperature aliquots were loaded onto the gel. b, Analysis of the marked bands with SDS-PAGE. The numbered boxes correspond to those in the BN-PAGE. As references, the transducer NpHtrII-157 and the receptor NpSRII are shown in lane 8 und 9, respectively.

conclusions that can be drawn from this experiment. (i) Solubilised NpSRII as well as NpHtrII do form homo-oligomers under these conditions (Figure 3(a), lanes 2, 9 and 10). This has been verified by extracting selected bands (numbered boxes) and subjecting them to gel electrophoresis (Figure 3(b)). For example an oligomer of NpSRII (box 7) displays in SDS solution only one band at the same position as the monomeric receptor (Figure 3(b), boxes 5 and 7). (ii) The binding of the transducer in a stoichiometry of about 1:1 can be deduced from lanes 3 to 5 (Figure 3(a)) and lanes 2 and 3 of Figure 3(b). At a mixing ratio of 1:1 only a small band of NpSRII is discernible, which becomes pronounced at a ratio of 2:1. The new bands appearing at 50 kDa (see e.g. Figure 3(a), box 2) correspond to the complex between HtrII-157 and NpSRII. This was proven in the gel, where these bands split into those of their parent molecules (Figure 3(b), boxes 2 and 3). (iii) Since the concentration of NpSRII was kept

constant (10 μM), it appears that NpHtrII-157 and NpSRII form a tighter complex than the homo-oligomers. This becomes clear if e.g. lane 4 is compared to lanes 2 and 9. In lane 4 the bands of the oligomers of NpSRII and NpHtrII-157 are not present. Similar experiments were done with the other shortened transducers. However, only NpHtrII-114 showed similar properties to NpHtrII-157, whereas for NpHtrII-101 and NpHtrII-82 no binding could be shown under these conditions.

In order to analyse whether polar interactions are important to form the complex, further BN-PAGE experiments were done with varying NaCl concentrations (data not shown). However, an effect of the ionic strength on the dimerisation and heterocomplex formation was not observed.

Isothermal titration calorimetry

In another set of experiments the binding affinities of the shortened transducer fragments to NpSRII were determined by using isothermal titration calorimetry (ITC). In these experiments the transducer fragments NpHtrII-157 and NpHtrII-114 were thermostatted at 45 °C, NpHtrII-101 and NpHtrII-82 at 22 °C and NpSRII was added in increments of 10 μl by a syringe. Figure 4

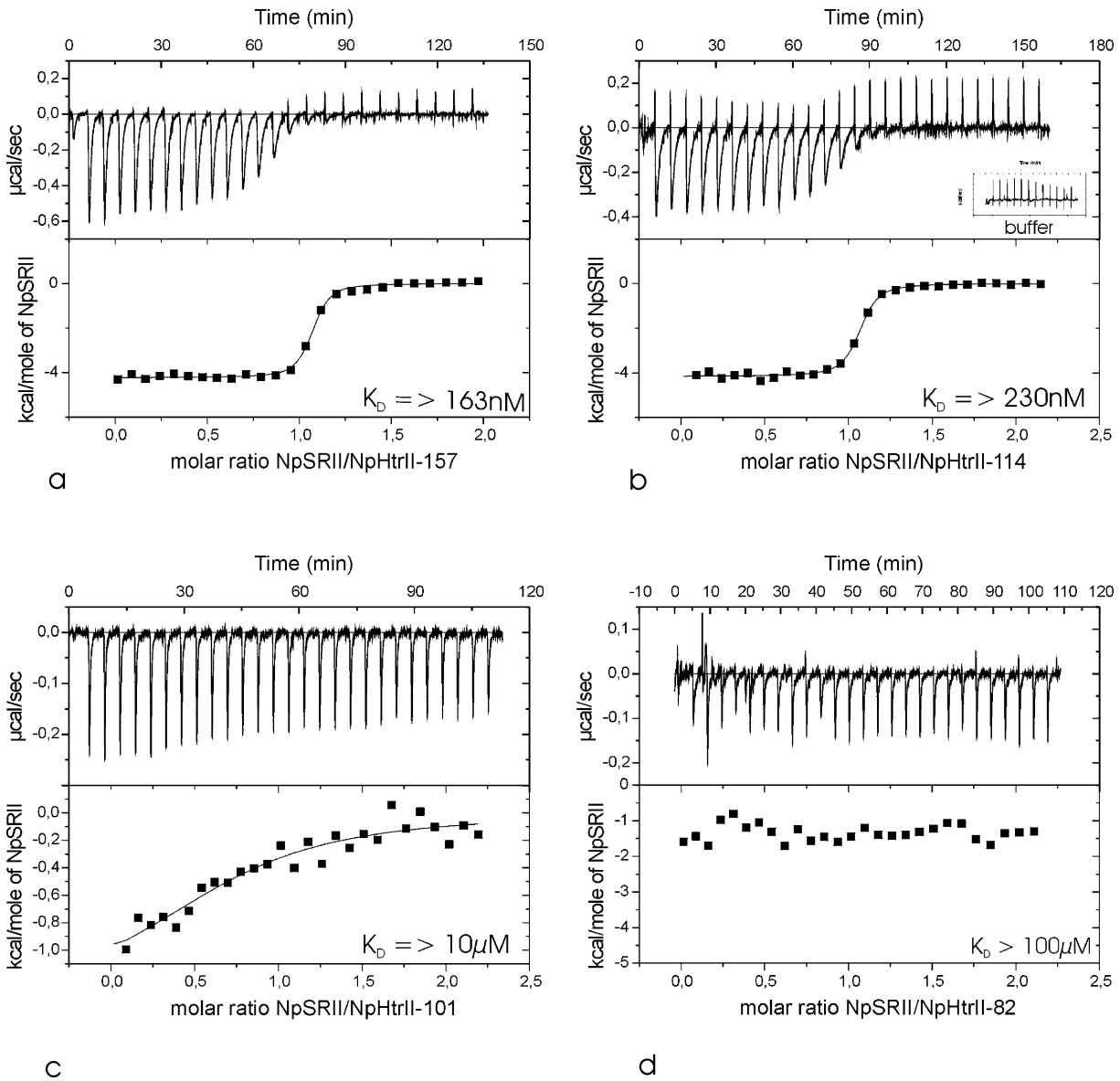

Figure 4. Isothermal calorimetric titration curves of NpSRII with NpHtrII-157 (a), NpHtrII-114 (b), NpHtrII-101 (c) and NpHtrII-82 (d). The upper panels represent the raw data after baseline correction. The small endothermal signal at the end of each titration is due to the mixing of NpSRII with detergent-containing buffer as shown in the inset of b. This overshoot is not resolved in the case of the NpHtrII-101 and NpHtrII-82 (c and d) because it is compensated by the exothermal reaction. In the lower panels the enthalpy changes per mole are plotted as a function of the molar ratio of receptor to transducer fragments. For the shortest fragment no binding was detectable. Taking the concentration of the NpHtrII fragments within the sample cell (~100 μM) into account it can be estimated that its $K_d \geq 100$ μM.

Table 1. Thermodynamic parameters of the association of NpHtrII fragments to NpSRII

NpHtrII	C_{NaCl} (mM)	pH	T (K)	$\Delta H°$ (kJ mol^{-1})	K_{ass} (M^{-1} × 10^6)	ΔG (kJ mol^{-1})	$\Delta S°$ (J mol^{-1}K^{-1})	K_D (nM)
157	150	8	318	−17.9	6.2	−41.35	73.74	160
114	150	8	318	−17.6	4.32	−40.38	71.16	240
101	150	8	295	−5.8	0.1	−28.23	76.20	10^4
82	150	8	295		< 0.01	–	–	$>10^5$

The measurements were performed at 45 °C for NpHtrII-157 and NpHtrII-114, and at 22 °C for NpHtrII-101 and NpHtrII-82 in degassed buffer containing 150 mM NaCl, 10 mM Tris (pH 8), 0.05% DDM.

shows the titration curves of NpSRII with the different transducer fragments. Measurements of the shorter transducers were performed at 22 °C because there aggregate at temperatures over 40 °C. Measurements of the longer transducer fragments displayed no detectable effect at lower temperature. The effect of temperature on the binding constants is neglectable in this case, as indicated by the van't Hoff equation. However, the reactions of NpSRII with the transducer fragments at 45 °C are exothermic with $\Delta H = -17.9$ kJ mol^{-1} for NpHtrII-157 and $\Delta H = -17.6$ kJ mol^{-1} for NpHtrII-114. NpHtrII-101 has a significantly decreased heat of formation ($\Delta H = -5.8$ kJ mol^{-1}), whereas the smallest transducer fragment showed neither release nor uptake of heat. The two longer NpHtrII fragments exhibit a stoichiometry of 1:1 (Figure 4(a) and (b)). For NpHtrII-101 $n = 0.75$ was found. Taking the signal to noise ratio of this latter measurement into account, a stoichiometry of 1:1 for this transducer fragment seems reasonable. The dissociation constants for the two longer fragments are almost identical in the range of 200 nM. However, the K_d of the smaller fragment NpHtrII-101 is increased by almost two orders of magnitude (10 μM), indicating that the sequence between 101 and 114 harbours an important motif for the receptor–transducer interaction. The results are summarised in Table 1.

To get more information about the nature of the complex binding, ITC experiments at different NaCl concentrations and pH values were performed. For these experiments the NpSRII and NpHtrII-157 were dialysed overnight against buffer with appropriate NaCl concentrations or pH values (ranging from 1 mM to 300 mM, pH 5, 6 and 8). The results are summarised in Table 2. As is obvious from these data, no significant influence of the ionic strength on the binding properties can be detected. Further experiments carried out at pH 6 revealed comparable results to those done at pH 8 (Table 2), whereas at pH 5 protein aggregation is observed obstructing the measurements. In order to elucidate whether specific amino acids from the membranous binding interface interfere with the proper binding of NpSRII to NpHtrII-157, site-directed mutants of Tyr199^{NpSRII} and Phe28^{NpHtrII} were prepared. These sites were chosen because data from EPR[20] and the crystal structure of NpSRII[16] indicate their juxtaposition. The crystal structure of the complex[17] confirmed this assumption, showing Tyr199 to be involved in a hydrogen bond with Asn74 of the transducer and Phe28 to comprise a major part of a tight binding pocket for Tyr199. Replacing Tyr199^{NpSRII} by Phe does not alter the binding properties significantly. The dissociation constant is still in the 200 nM range and the thermodynamic data remain unaltered within the error limit as compared to the wild-type (Table 3). A different picture emerges if Tyr199^{NpSRII} and/or Phe28^{NpHtrII} are changed to Ala. In this case no binding is observed ($K_d > 100\ \mu M$). It can be concluded that the hydrogen bond formed between Tyr199^{NpSRII} and Asn74^{NpHtrII} (located on TM2), is not necessary for a tight binding of the transducer to the receptor. On the other hand, the aromatic side-chains of Tyr199^{NpSRII} and Phe28^{NpHtrII} are essential for proper binding.

Table 2. Thermodynamic parameters of the binding of NpHtrII-fragments to NpSRII in dependence of pH and ionic strength

NpHtrII	C_{NaCl} (mM)	pH	T (K)	$\Delta H°$ (kJ mol^{-1})	K_{ass} (M^{-1} × 10^6)	ΔG (kJ mol^{-1})	$\Delta S°$ (J mol^{-1}K^{-1})	K_D (nM)
157	150	6	318	−20.0	9.98	−42.61	71.10	100
114	1	8	318	−25.8	3.13	−39.56	43.27	320
114	10	8	318	−17.6	4.20	−40.33	71.48	240
114	15	8	318	−26.0	2.97	−39.40	42.14	340
114	50	8	318	−26.0	4.85	−40.72	46.28	210
114	100	8	318	−15.2	4.41	−40.46	79.43	230
114	150	8	318	−17.6	4.21	−40.32	71.44	230
114	300	8	318	−21.5	9.37	−42.44	65.84	110

The measurements were performed at 45 °C in degassed buffer containing different NaCl-concentrations, 10 mM Tris (pH 8) and 0.05% DDM.

Table 3. Binding properties of NpHtrII-157 to NpSRII mutants

NpSRII residue at position 199	NpHtrII-157 residue at position 28	K_D (μM)	$\Delta H°$ (kJ mol^{-1})	K_{ass} ($M^{-1} \times 10^6$)	ΔG (kJ mol^{-1})	$\Delta S°$ (J mol^{-1}K^{-1})
Tyr (wt)	Ala	>100	–	–	–	–
Phe	Phe (wt)	0.3	−22.6	3.2	−39.62	53.52
Phe	Ala	>100	–	–	–	–
Ala	Phe (wt)	>100	–	–	–	–

Photocurrent measurements

In previous work it was shown that in the NpSRII/NpHtrII, like in the HsSRI/HsHtrI complex the light-activated proton pump is blocked.[3,21,22] Schmies and co-workers demonstrated this property of the transducer by voltage clamping NpSRII-F86D-NpHtrII expressing oocytes.[22] In the present work advantage is taken of the observation, that the NpSRII-F86D mutant displays a considerable larger photostationary current than the wild-type. The reason for the difference in pump efficiency is due to a two-photon process, which shortcuts the slow photocycle kinetics.[13] The mRNA of NpSRII-F86D (15 ng) was injected without or together with excess mRNA (50 ng) of the transducer fragments NpHtrII-82, NpHtrII-101, NpHtrII-113, and NpHtrII-159 into oocytes. After an incubation period of about three days the photocurrent was measured (applied voltage = −40 mV, filter 50 Hz). The results are presented in Figure 5 (data for NpHtrII-159 are not shown).

Continuous light induces a stationary current in oocytes expressing NpSRII-F86D, which is typically preceded by a transient current (see Figure 5(a)). The absence of the transient photocurrent in some of the other traces (e.g. Figure 5(b)) might be due to non-saturating light conditions in which the absorption of photons becomes rate-limiting. For irradiated oocytes, expressing the receptor together with the full-length transducer, the photostationary current is inhibited and only the transient current remains (Figure 5(e)[22]). Similarly, on addition of the longer transducer fragments 1–113 (Figure 5(h)) and 1–159 (data not shown) a stationary current cannot be detected. However, in the case where NpSRII-F86D is expressed with one of the shorter fragments 1–82 and 1–101, both transient and stationary currents are observed (Figure 5(f) and (g)).

The observation that the transient photocurrent is still present, even if the transducer or one of its longer fragments (1–113 or 1–159) is bound to NpSRII, indicates that the first part of the photocycle including the deprotonation of the Schiff base is unimpaired. The inhibition of the stationary photocurrent, however, suggests that the uptake of a proton from the cytoplasm, which is temporally linked to the M-decay and the reformation of the original state, is blocked. The peptide site, which

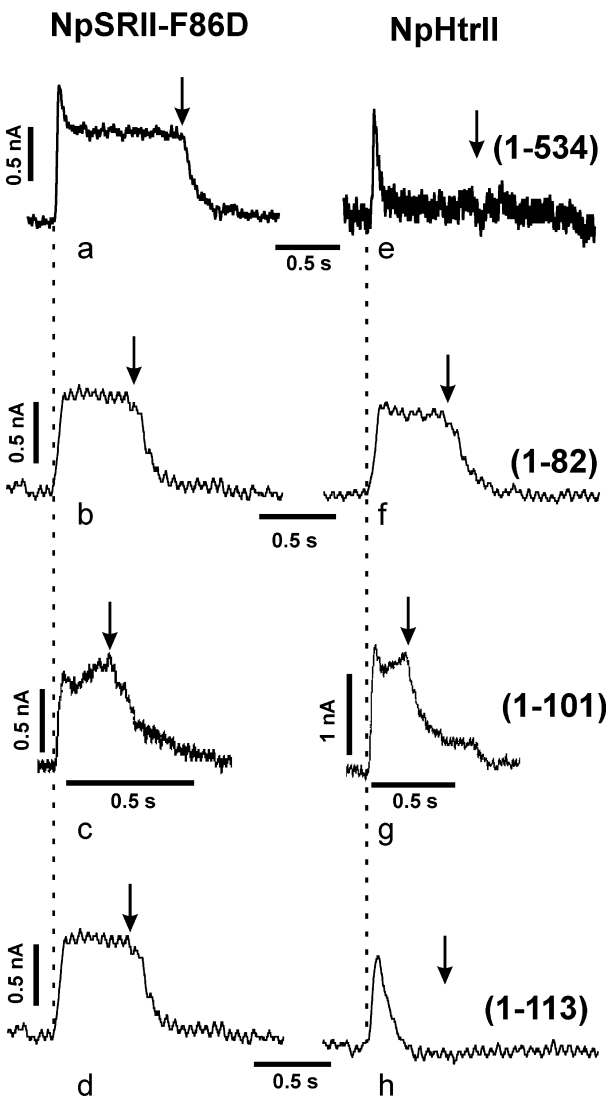

Figure 5. Photocurrents of NpSRII/transducer expressing oocytes. The left column represents the measurements with oocytes expressing NpSRII-F86D, the right column those oocytes expressing both NpSRII-F86D and a transducer fragment (as indicated). In these experiments the oocytes were injected with either 15 ng of mRNA NpSRII-F86D + H_2O (a–d) or 15 ng of NpSRII-F86D and 50 ng of NpHtrII (e), NpHtrII-82 (f), NpHtrII101 (g) or NpHtrII-113 (h). The samples were irradiated with orange light (dotted line, light on; black arrow, light off).

interferes with the proton uptake, has to be located between amino acid residues 102 and 113 because the transducer fragment 1–101 is not able to block the proton pump but the fragment 1–113 does inhibit the proton transfer.

Discussion

The results presented above contain two main aspects, which will be discussed. The first point relates to the size of the receptor-binding domain of the transducer in the NpSRII/NpHtrII complex. In the recently published structure of the NpSRII/NpHtrII complex the whole domain was not completely resolved.[17] The results presented here shed light on the structure and size of the receptor-binding domain. Secondly, of more general interest are those experiments that provide information about the thermodynamics and kinetics of the transducer binding. As these data have been notoriously difficult to determine for membrane proteins, the present results provides a new approach to study these interactions.

Receptor binding domain

There are two lines of evidence from which it can be concluded that the receptor binding domain comprises maximally the first 114 amino acid residues. The association constant of this fragment to the receptor is $4.2 \times 10^6\ M^{-1}$, only slightly smaller than that of the longer fragment 1–157 ($6.2 \times 10^6\ M^{-1}$). However, reducing the length of the transducer further to 101 amino acid residues decreases the binding constant by a factor of 40 ($0.1 \times 10^6\ M^{-1}$). This observation is supported by the data obtained from the photocurrent measurements. Whereas 1–113 is still capable of blocking the light-activated proton pump of NpSRII-F86D, the fragment 1–101 is not inhibiting the proton transfer across the membrane. Reducing the length of NpHtrII even further abolishes the capability of the transducer to bind to the receptor ($K_D > 100\ \mu M$). Apparently, the peptide 83–114 comprises an essential part of the receptor-binding domain. The property to block the proton pump activity of NpSRII is conferred by the small peptide 101–114, which also completes the tight binding as observed for the longer fragment 1–157. The consistency of the data obtained by the two methods shows that the His-tag fused to the shortened transducer fragments (1–114 and 1–157) for the ITC experiments does not significantly influence the association constants.

From these results and those obtained from the crystal structure of the complex[17] it is possible to define the receptor binding site of the transducer, which comprises the two transmembrane helices TM1 and TM2 as well as the cytoplasmic peptide 83–114.

The sequence of the peptide 101–114 (^{101}GDG DLDVELETRRE^{114}) is highly charged including six negative and two positive charges. In HsHtrII from *H. salinarum*, four of the acidic and one of the basic groups are conserved,[27] whereas the corresponding sequence of SRI does not show this charged imprinting.[28] It seems, therefore, possible that the interface between this peptide and NpSRII is governed by electrostatic interactions as was proposed by Royant *et al.*[18] for ^{101}GDGDLD with a positive patch close to helix F. However, in order to inhibit the proton pump the peptide should block the proton uptake channel, since the structure of NpSRII, whether bound or not bound to the transducer, is with few exceptions not altered.[17] Indeed positive charges are close to the channel, which might interact with Glu and Asp of the peptide, thereby disturbing the proton uptake from the bulk. However, a cautionary note is necessary because amino acid residues responsible for the surface charge of NpSRII are not conserved in both HsSRII[27] and vSRII.[29] Furthermore, the high ionic strength found in the natural environment of *N. pharaonis* does not favour electrostatic interactions. Indeed, the experiments described above do not indicate a dependency of the binding constant on ionic strength.

This view is supported by the results obtained from the mutation studies. The exchange of the two aromatic amino acids, one on TM1 (Phe28^{TM1}) the other on helix G (Tyr199^{G}) by Ala destroys the capability of NpHtrII to bind to NpSRII (Table 3). The replacement of Tyr199 by Phe (Tyr199Phe) does not influence the binding as indicated by the "native-like" dissociation constant. Obviously, the hydrogen bond between the phenolic group of Tyr199 to Asn74 (TM2)[17] is not crucial but the aromatic side-chain is essential for selective

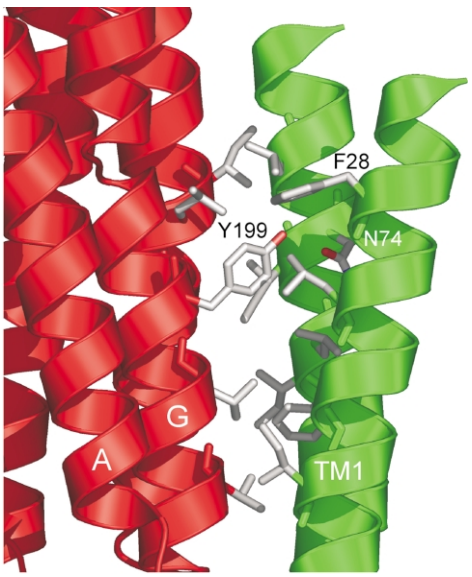

Figure 6. Section of the NpSRII/NpHtrII complex structure[17] showing the binding interface between the respective transmembrane helices. NpSRII helices are depicted as red ribbons, NpHtrII helices in green. Important side-chains are labelled.

binding. It should be noted, that Kamo and co-workers concluded from photocycle data that the replacement of Tyr199 by Phe or by Val affects K_D by a factor of 10.[30] The crystal structure of the complex[17] reveals a tight intercalation of the aromatic side-chains between residues located on the partner molecule (Figure 6). It seems possible that $Phe28^{TM1}$ and $Tyr199^{G}$ not only confer binding energy by van der Waals forces but that they might also function as steering points directing the two molecules into a position for optimal and functionally relevant interactions.

It is interesting to compare these data with those gained by other groups mostly from studies on SRI/HtrI from *H. salinarum*[31–33] but also on NpSRII/NpHtrII.[34] Spudich and co-workers demonstrated that a minimal fragment (1 − 147) of the HtrI transducer leaves the wild-type pH-insensitive photocycle unaffected.[32] Obviously, the receptor-binding domain of HtrI seems to be more extended than that of NpHtrII, an observation however, which has to be further investigated. In the case of the NpSRII/NpHtrII protein complex Jung *et al.* constructed fusion proteins in which the cytoplasmic domain of NpHtrII was replaced by the corresponding domains of Tar and Tsr, chemotaxis receptors from enteric eubacteria.[34] The smallest NpHtrII fragment, still showing a "weak repellent" phototaxis response comprised residues 1–102. In the present study this fragment displayed a reduced association constant and the proton pump activity of NpSRIIF86D was not inhibited (Table 4). The results from both studies indicate that the property of NpHtrII to inhibit the proton pump of the receptor is not necessarily coupled to its capability for transferring the signal from the transmembrane to the signalling domain. Regardless of whether the proton transfer reactions are required for signal transduction, the influence of the transducer on the proton translocation is a measure of the formation of the NpSRII/NpHtrII complex.

Thermodynamics of receptor–transducer association

The lateral association of membrane proteins to form a functional complex has only been elucidated in a few examples. Especially, quantitative thermodynamic information of membrane protein assembly is mostly lacking due to the special nature of this protein family. Accordingly, only a few data are available to date, which were primarily gained by using sedimentation equilibrium analytical ultracentrifugation (reviewed by Fleming[35]). In a well examined example the dimerisation of glycophorin A monomers was studied.[36,37] The formation of homodimers in the presence of the detergent C_8E_5 occurred with a $K_D = 220$ nM. ΔG of this reaction was determined to be $-38\ kJ\ mol^{-1}$.[36] In another publication Engelman and co-workers determined the Gibbs free energy to be $32\ kJ\ mol^{-1}$ with 50% entropic contribution ($\Delta S = 50\ J\ mol^{-1}\ K^{-1}$) to this reaction in the detergent SDS.[38] The detergent concentration quite sensitively influences the dissociation constants, and under these conditions K_D is increased to 2.7 μM. Obviously, the nature of the detergent is an important factor for the thermodynamics of membrane–protein interactions.

The present thermodynamic data were obtained by using ITC, a method not used so far for the study of membrane proteins. As pointed out above the data do not necessarily mirror the situation in native membranes and the association constants and ΔH measured might represent minimal values because the proteins as purified form multimers and only on binding to the partner molecule do these aggregates dissolve (Figure 2). Despite these restrictions the data provide some important results on membrane–protein interactions. The dissociation constant of NpSRII and the shortened transducer is in the 100 nM range similar to the glycophorin A system[36] but also to interactions of soluble proteins like e.g. those measured for the Ras/RBD protein pair.[39] It is also interesting to note that the association of NpSRII with NpHtrII occurs with higher K_{ass} than that of the heterodimers, since the original tetrameric form occurs only in membranes but not when solubilised in detergents.[20] An interesting aspect concerns the mutations in TM1 of the transducer (F28A) and helix G of the receptor (Y199F,A). As pointed out above, the hydrogen bond that is formed between the phenolic group of Tyr199 and Asn74 (TM2) has just minor influence on the energetics of the association. The absence of this hydrogen bond in NpSRII-Y199F decreases the amount of the free energy (ΔG) of binding by just about $1.73\ kJ\ mol^{-1}$. Usually, the formation of a hydrogen bond in a hydrophobic environment is favoured by about $15–25\ kJ\ mol^{-1}$.[40] Here, the removal of the hydroxyl group increases the enthalpic portion of the free energy (ΔH) by about $4.7\ kJ\ mol^{-1}$, whereas the entropic term contributes $17.02\ kJ\ mol^{-1}$ instead of $23.44\ kJ\ mol^{-1}$ observed for the native transducer fragment.

Replacing the aromatic amino acids by the smaller Ala completely abolishes the association of the transducer to the receptor. As pointed out above, the reason for this drastic effect could be the decreased packing at the dimer interface. Fleming *et al.*[36] made a similar observation, though not as extreme. Replacing the bulky Leu or Ile by Ala in glycophorin A decreased the dissociation

Table 4. Summary of the binding properties of the different transducer fragments with the corresponding results of the electrophysiological measurements

Transducer-fragment	K_D	Stationary photocurrent
NpHtrII-82	>100 μM	Yes
NpHtrII-101	~10 μM	Yes
NpHtrII-114/113	230 nM	No
NpHtrII-157/159	160 nM	No

constant from $K_D = 240$ nM to $K_D = 1.7$ μM. The question arises why the single-site mutants Tyr199-Ala^{NpSRII} or Phe28Ala^{NpHtrII} but also the small fragment NpHtrII-82, comprising only the two transmembrane helices, abolish the formation of a tight complex. An answer might be, that a synergistic interplay of the transducer transmembrane domain (1–82) with the cytoplasmic peptide (83–114) leads to an optimal and specific complexation.

The elucidation of membrane–protein interaction and transmembrane signal transduction requires structural and thermodynamical information about these processes. In this work calorimetric and electrophysiological techniques were applied, which confined the receptor-binding site of the transducer and provided information about the strength and energetics of the binding process. This latter information is of general interest because it could be shown that ITC is a suitable method to study directly membrane protein/protein interactions, which, although performed in a micelle environment, will enlarge our knowledge about this class of proteins.

Material and Methods

Cloning and expression

Bacterial strains

As a host for DNA manipulations *Escherichia coli* XL1-Blue was used. Gene expression was carried out in *E. coli* BL21 (DE3). Cells were grown in Luria–Bertani medium containing 50 μg/ml of kanamycin.

Cloning and expression of NpHtrII variants

Different NpHtrII constructs from residues 1–157 (NpHtrII-157), 1–114 (NpHtrII-114), 1–101 (NpHtrII-101) and 1–82 (NpHtrII-82) were prepared by polymerase chain reaction. The DNA sequence coding for the NpHtrII-157 fragment was amplified using the NpHtrII genomic sequence[29] as a template. 5′-*Nco*I/3′-*Eco*RI restriction sites are introduced to facilitate the subcloning into pET27bmod[41] in-frame with a C-terminal additional His-tag obtaining the plasmid pET27bmod-nphtrII$_{157}$-His. The DNA sequences coding for the truncated transducer molecules were constructed in the same way using pET27bmod-nphtrII$_{157}$-His as a template. Due to introduction of an *Nco*I site, Ser2 is changed to Ala, resulting in the N-terminal sequence ^{1}MALNV….

The coding sequences were confirmed by DNA sequencing. The resulting plasmids were used for transformation of *E. coli* BL21(DE3) as an expression strain. Expression and purification of the transducer variants followed essentially the protocol described for the co-expression with NpSRII.[19] Due to the low fraction of aromatic amino acids in the truncated fragments (NpHtrII) ($\varepsilon_{280}^{calc} = 3000$ cm l/mol) and the perturbation of dye-assays by detergents, protein concentration is determined measuring the absorbance at 205 nm,[42] where $A = 31$ equals a concentration of 1 mg protein/ml. Alternatively, an empirical equation $c_{NpHtrII}(mg/ml) = A_{228.5} - A_{234.5}/3.14$, which is based on the absorption at 228.5 nm ($A_{228.5}$) and 234.5 nm ($A_{234.5}$), was used to determine the NpHtrII concentration ($c_{NpHtrII}$).[43] Expression and purification of NpSRII was carried out as described.[25]

NpSRII mutants

Starting with the plasmid pET27bmod-npsopII-His[25] the single-site mutations Y199A and Y199F were introduced using a PCR procedure according to the overlap extension method.[44] The final PCR products were ligated *via* *Nco*I and *Hin*dIII into the vector pET27bmod. The correct sequences of the final npsopII-Y199A-His and npsopII-Y199F-His genes were confirmed by DNA sequencing.

Gel electrophoresis

BN-PAGE was performed as outlined by Schägger & Jagow[26] using a discontinuous system with 4% (w/v) acrylamide in the stacking gel followed by a 10–20% gradient for separation. Prior to the electrophoresis the solubilised NpSRII and the truncated NpHtrIIs are incubated together for one hour at room temperature. Using the system Hoefer® SE-400 (Pharmacia) the electrophoresis conditions were 150 V, 25 mA and 20 W for accumulation of samples in the stacking gel. Voltage was then set to 500 V with the current limited to 15 mA for separation at 4 °C. Selected bands from the BN-PAGE were ground to small pieces, and incubated for 15 minutes at 40 °C in SDS-buffer. The supernatant was analysed by SDS-PAGE.

Isothermal titration calorimetry

Isothermal titrations were carried out using an automated OMEGA titration calorimeter (MicroCal, USA). Concentrated protein solutions of solubilised NpSRII (700–1000 μM) and NpHtrII (70–100 μM) were dialysed at 4 °C overnight against degassed buffer containing 150 mM NaCl, 10 mM Tris (pH 8), 0.05% (w/v) *n*-dodecyl-β-D-maltopyranoside (DDM) (v/v = 1/2000). NpSRII (250 μl) was titrated in 10 μl steps (interval time five minutes) into a solution of NpHtrII (1.4 ml). Titrations were carried out at 22 °C and 45 °C. For control experiments detergent-containing buffers were used (1% DDM, syringe; 0.1% DDM, chamber) to be sure that there is no effect due to the detergent. Futhermore control experiments were done after every set of measurements using protein samples (NpSRII or its mutants) in the syringe (0.05% DDM) and only buffer (0.05% DDM) in the chamber. Data are evaluated employing the software package Origin-ITC.

Plasmids and mRNA synthesis

For the *in vitro* synthesis of the mRNA, the vector pNK4 was used.[45] All genes were cloned into pNK4 as described by Schmies *et al.*[22] by *Nco*I and *Xho*I digestion of the corresponding plasmids derived from pET27bmod.[46] Truncated NpHtrII-159 was obtained similarly by cloning the *Nco*I-*Xho*I fragment from plasmid pET27bmod-nphtrII-His[20] into the vector pNK4. The pNK4 vector is suitable for the synthesis of mRNA containing a 3′ poly(A) tail and a 5′ sequence encoding the ribosomal binding site of the β-subunit of the *Xenopus laevis* Na/K ATPase. For the mRNA

synthesis (SP6-mMessagemMachine kit; Ambion, Austin, TX) the *Xba*I-linearised DNA was used.

The synthesis of the shortened transducer molecules was carried out by PCR[44] using an appropriate mutagenesis primer, which introduced two stop codons (TAA-TGA) at positions adjacent to the codon of L82, G101 and R113.

Oocyte microinjection and voltage clamp measurements

Xenopus oocytes have been isolated using the procedure described by Grygorczyk *et al*.[47] If not otherwise noted, for the expression of NpSRII, oocytes were injected with 15 ng of mRNA. In the case of co-expression of NpSRII/NpHtrII complexes, 50 ng of mRNA of NpHtrII and its shortened analogues were additionally injected. The oocytes were incubated for three to five days at 18 °C in the presence of 1 μM all-*trans* retinal.

The voltage clamp measurements were performed as described.[23,48] The membrane potential was clamped at −40 mV if not otherwise noted (50 Hz signal filtering). The bath solution was 90 mM NaCl, 5 mM $BaCl_2$, 20 mM tetraethylammonium (TEA)–Hce, 10 mM Mops (pH 7.6).

Acknowledgements

We thank M. Schumacher for excellent technical help, and the Deutsche Forschungsgemeinschaft and the Max Planck Gesellschaft for financial support. G.S. acknowledges a fellowship by the Boehringer Ingelheim Fonds.

References

1. Takahashi, T., Tomioka, H., Kamo, N. & Kobatake, Y. (1985). A photosystem other than PS370 also mediates the negative phototaxis of *Halobacterium halobium*. *FEMS Microbiol. Letters*, **28**, 161–164.
2. Schäfer, G., Engelhard, M. & Müller, V. (1999). Bioenergetics of the archaea. *Microbiol. Mol. Biol. Rev.* **63**, 570–620.
3. Sasaki, J. & Spudich, J. L. (2000). Proton transport by sensory rhodopsins and its modulation by transducer-binding. *Biochim. Biophys. Acta*, **1460**, 230–239.
4. Lanyi, J. K. (2000). Molecular mechanism of ion transport in bacteriorhodopsin: insights from crystallographic, spectroscopic, kinetic, and mutational studies. *J. Phys. Chem. B*, **104**, 11441–11448.
5. Haupts, U., Tittor, J. & Oesterhelt, D. (1999). Closing in on bacteriorhodopsin: progress in understanding the molecule. *Annu. Rev. Biophys. Biomol. Struct.* **28**, 367–399.
6. Spudich, J. L. (1998). Variations on a molecular switch—transport and sensory signalling by archaeal rhodopsins. *Mol. Microbiol.* **28**, 1051–1058.
7. Hou, S. B., Brooun, A., Yu, H. S., Freitas, T. & Alam, M. (1998). Sensory rhodopsin II transducer HtrII is also responsible for serine chemotaxis in the archaeon *Halobacterium salinarum*. *J. Bacteriol.* **180**, 1600–1602.
8. Falke, J. J., Bass, R. B., Butler, S. L., Chervitz, S. A. & Danielson, M. A. (1997). The two-component signaling pathway of bacterial chemotaxis—a molecular view of signal transduction by receptors, kinases, and adaptation enzymes. *Annu. Rev. Cell Develop. Biol.* **13**, 457–512.
9. Stock, A. M., Robinson, V. L. & Goudreau, P. N. (2000). Two-component signal transduction. *Annu. Rev. Biochem.* **69**, 183–215.
10. Hoff, W. D., Jung, K. H. & Spudich, J. L. (1997). Molecular mechanism of photosignaling by archaeal sensory rhodopsins. *Annu. Rev. Biophys. Biomol. Struct.* **26**, 223–258.
11. Marwan, W. & Oesterhelt, D. (2000). Archaeal vision and bacterial smelling: Sensory Control of the swimming behavior by two component signaling and fumarate. *ASM-News*, **66**, 83–89.
12. Chizhov, I., Schmies, G., Seidel, R., Sydor, J. R., Lüttenberg, B. & Engelhard, M. (1998). The photophobic receptor from *Natronobacterium pharaonis*—temperature and pH dependencies of the photocycle of sensory rhodopsin II. *Biophys. J.* **75**, 999–1009.
13. Sasaki, J. & Spudich, J. L. (1999). Proton circulation during the photocycle of sensory rhodopsin II. *Biophys. J.* **77**, 2145–2152.
14. Iwamoto, M., Shimono, K., Sumi, M., Koyama, K. & Kamo, N. (1999). Light-induced proton uptake and release of pharaonis phoborhodopsin detected by a photoelectrochemical cell. *J. Phys. Chem. ser. B*, **103**, 10311–10315.
15. Schmies, G., Lüttenberg, B., Chizhov, I., Engelhard, M., Becker, A. & Bamberg, E. (2000). Sensory rhodopsin II from the haloalkaliphilic *Natronobacterium pharaonis*: light-activated proton transfer reactions. *Biophys. J.* **78**, 967–976.
16. Luecke, H., Schobert, B., Lanyi, J. K., Spudich, E. N. & Spudich, J. L. (2001). Crystal structure of sensory rhodopsin II at 2.4 Ångstroms: insights into color tuning and transducer interaction. *Science*, **293**, 1499–1503.
17. Gordeliy, V. I., Labahn, J., Moukhametzianov, R., Efremov, R., Granzin, J., Schlesinger, R. *et al.* (2002). Molecular basis of transmembrane signalling by sensory rhodopsin II-transducer complex. *Nature*, **419**, 484–487.
18. Royant, A., Nollert, P., Neutze, R., Landau, E. M., Pebay-Peyroula, E. & Navarro, J. (2001). X-ray structure of sensory rhodopsin II at 2.1-Å resolution. *Proc. Natl Acad. Sci. USA*, **98**, 10131–10136.
19. Wegener, A. A., Chizhov, I., Engelhard, M. & Steinhoff, H. J. (2000). Time-resolved detection of transient movement of helix F in spin-labelled pharaonis sensory rhodopsin II. *J. Mol. Biol.* **301**, 881–891.
20. Wegener, A. A., Klare, J. P., Engelhard, M. & Steinhoff, H. J. (2001). Structural insights into the early steps of receptor-transducer signal transfer in archaeal phototaxis. *EMBO J.* **20**, 5312–5319.
21. Sudo, Y., Iwamoto, M., Shimono, K., Sumi, M. & Kamo, N. (2001). Photo-induced proton transport of pharaonis phoborhodopsin (sensory rhodopsin II) is ceased by association with the transducer. *Biophys. J.* **80**, 916–922.
22. Schmies, G., Engelhard, M., Wood, P. G., Nagel, G. & Bamberg, E. (2001). Electrophysiological characterization of specific interactions between bacterial sensory rhodopsins and their transducers. *Proc. Natl Acad. Sci. USA*, **98**, 1555–1559.
23. Nagel, G., Möckel, B., Büldt, G. & Bamberg, E. (1995). Functional expression of bacteriorhodopsin in

oocytes allows direct measurement of voltage dependence of light induced H^+ pumping. *FEBS Letters*, **377**, 263–266.
24. Shimono, K., Iwamoto, M., Sumi, M. & Kamo, N. (1997). Functional expression of pharaonis phoborhodopsin in *Escherichia coli*. *FEBS Letters*, **420**, 54–56.
25. Hohenfeld, I. P., Wegener, A. A. & Engelhard, M. (1999). Purification of histidine tagged bacteriorhodopsin, pharaonis halorhodopsin and pharaonis sensory rhodopsin II functionally expressed in *Escherichia coli*. *FEBS Letters*, **442**, 198–202.
26. Schägger, H. & von Jagow, G. (1991). Blue native electrophoresis for isolation of membrane protein complexes in enzymatically active form. *Anal. Biochem.* **199**, 223–231.
27. Zhang, W. S., Brooun, A., Mueller, M. M. & Alam, M. (1996). The primary structures of the archaeon *Halobacterium salinarium* blue light receptor sensory rhodopsin II and its transducer, a methyl-accepting protein. *Proc. Natl Acad. Sci. USA*, **93**, 8230–8235.
28. Blanck, A., Oesterhelt, D., Ferrando, E., Schegk, E. S. & Lottspeich, F. (1989). Primary structure of sensory rhodopsin I, a prokaryotic photoreceptor. *EMBO J.* **8**, 3963–3971.
29. Seidel, R., Scharf, B., Gautel, M., Kleine, K., Oesterhelt, D. & Engelhard, M. (1995). The primary structure of sensory rhodopsin II: a member of an additional retinal protein subgroup is coexpressed with its transducer, the halobacterial transducer of rhodopsin II. *Proc. Natl Acad. Sci. USA*, **92**, 3036–3040.
30. Sudo, Y., Iwamoto, M., Shimono, K. & Kamo, N. (2002). Tyr-199 and charged residues of pharaonis phoborhodopsin are important for the interaction with its transducer. *Biophys. J.* **83**, 427–432.
31. Krah, M., Marwan, W. & Oesterhelt, D. (1994). A cytoplasmic domain is required for the functional interaction of SRI and HtrI in archaeal signal transduction. *FEBS Letters*, **353**, 301–304.
32. Jung, K. H. & Spudich, J. L. (1996). Protonatable residues at the cytoplasmic end of transmembrane helix-2 in the signal transducer HtrI control photochemistry and function of sensory rhodopsin I. *Proc. Natl Acad. Sci. USA*, **93**, 6557–6561.
33. Perazzona, B., Spudich, E. N. & Spudich, J. L. (1996). Deletion mapping of the sites on the htrI transducer for sensory rhodopsin I interaction. *J. Bacteriol.* **178**, 6475–6478.
34. Jung, K. H., Spudich, E. N., Trivedi, V. D. & Spudich, J. L. (2001). An archaeal photosignal-transducing module mediates phototaxis in *Escherichia coli*. *J. Bacteriol.* **183**, 6365–6371.
35. Fleming, K. G. (2000). Probing stability of helical transmembrane proteins. *Methods Enzymol.* **323**, 63–76.
36. Fleming, K. G., Ackerman, A. L. & Engelman, D. M. (1997). The effect of point mutations on the free energy of transmembrane alpha-helix dimerization. *J. Mol. Biol.* **272**, 266–275.
37. Fleming, K. G. (2002). Standardizing the free energy change of transmembrane helix–helix interactions. *J. Mol. Biol.* **323**, 563–571.
38. Fisher, L. E., Engelman, D. M. & Sturgis, J. N. (1999). Detergents modulate dimerization, but not helicity, of the glycophorin A transmembrane domain. *J. Mol. Biol.* **293**, 639–651.
39. Sydor, J. R., Engelhard, M., Wittinghofer, A., Goody, R. S. & Herrmann, C. (1998). Transient kinetic studies on the interaction of ras and the ras-binding domain of c-raf-1 reveal rapid equilibration of the complex. *Biochemistry*, **37**, 14292–14299.
40. Allen, L. C. (1975). A model for the hydrogen bond. *Proc. Natl Acad. Sci. USA*, **72**, 4701–4705.
41. Klostermeier, D., Seidel, R. & Reinstein, J. (1998). Functional properties of the molecular chaperone DnaK from *Thermus thermophilus*. *J. Mol. Biol.* **279**, 841–853.
42. Scopes, R. K. (1974). Measurement of protein by spectrophotometry at 205 nm. *Anal. Biochem.* **59**, 277–282.
43. Ehresmann, B., Imbault, P. & Weil, J. H. (1973). Spectrophotometric determination of protein concentration in cell extracts containing tRNA's and rRNA's. *Anal. Biochem.* **54**, 454–463.
44. Ho, S. N., Hunt, H. D., Horton, R. M., Pullen, J. K. & Pease, L. R. (1989). Site-directed mutagenesis by overlap extension using the polymerase chain reaction. *Gene*, **77**, 51–59.
45. Gloor, S., Pongs, O. & Schmalzing, G. (1995). A vector for the synthesis of cRNAs encoding Myc epitope-tagged proteins in *Xenopus laevis* oocytes. *Gene*, **160**, 213–217.
46. Schmies, G., Chizhov, I. & Engelhard, M. (2000). Functional expression of His-tagged sensory rhodopsin I in *Escherichia coli*. *FEBS Letters*, **466**, 67–69.
47. Grygorczyk, R., Hanke-Baier, P. S. W. & Passow, H. (1989). Measurement of erythroid band 3 protein-mediated anion transport in mRNA-injected oocytes of *Xenopus laevis*. *Methods Enzymol.* **173**, 453–466.
48. Nagel, G., Kelety, B., Mockel, B., Büldt, G. & Bamberg, E. (1998). Voltage dependence of proton pumping by bacteriorhodopsin is regulated by the voltage-sensitive ratio of M-1 to M-2. *Biophys. J.* **74**, 403–412.

Edited by G. von Heijne

(Received 14 March 2003; received in revised form 14 May 2003; accepted 15 May 2003)